Inclusive 150-MeV-proton-induced spectra at forward angles

R. E. Segel, S. M. Levenson, P. Zupranski,* A. A. Hassan, and S. Mukhopadhyay
Department of Physics and Astronomy, Northwestern University, Evanston, Illinois 60201

J. V. Maher
Physics Department, University of Pittsburgh, Pittsburgh, Pennsylvania 15260
(Received 27 September 1984)

Inclusive proton spectra were measured from the interaction of 150 MeV protons with a variety of targets ranging from berylium to bismuth over the angular range from 10° to 30°. At all of the angles at which data were taken the spectra from the berylium and the carbon targets show strong peaks attributable to quasifree scattering while the spectra from nickel and heavier targets are rather flat throughout the continuum region. The quasifree scattering is calculated using a Fermi gas model, with the nucleus a uniform sphere, and in this picture the required attenuation of a quasifree peak requires a nucleon free path of no more than about 3.5 fm. Spectra of deuterons, tritons, ^{3}He, and alpha particles were also measured.

INTRODUCTION

At incident nucleon energies above 100 MeV it is expected that nucleon-nucleus reactions can be described as a series of nucleon-nucleon reactions within the nucleus. Exceptions would be elastic scattering and inelastic scattering to excited states of the target nucleus, both of which can be said to involve the target nucleus as a whole, but these constitute only a tiny fraction of the total reaction cross section. Thus, from the elementary nucleon-nucleon cross sections, it should be possible to calculate the various nucleon-nucleus reaction cross sections. The simplest nucleon-nucleus reaction is quasifree scattering, in which the incident nucleon scatters off a single nucleon in the nucleus. Attempts to calculate quasifree scattering and compare the results with experiment soon run into both theoretical and experimental uncertainties and it is the purpose of the present work to try to remove some of these uncertainties.

Experimentally, the main source of confusion appears to be a paper by Wall and Roos[1] which reported strong quasifree peaks in inclusive proton spectra over a wide range of targets and angles for 160 MeV incident protons. Two other papers,[2,3] also published in the late sixties, reported much less peaking, thus disagreeing with Wall and Roos. More recently, Chen *et al.*[4,5] at 164 MeV found little evidence for quasifree peaks at angles of 25° or more for targets ranging from Al to Pb. A recent experiment by Machner *et al.*[6] reports agreement with Chen *et al.*[4,5] and disagreement with Wall and Roos.[1] It thus appears to be established that for incident proton energies up to about 200 MeV inclusive proton spectra do not contain strong quasifree peaks, at least for targets with A of about 60 or greater, and at angles of about 25° or more. A major purpose of the present work is to complete the delineation of the role of quasifree scattering in the 150–200 MeV region by extending the measurements down to smaller angles where, it is shown below, the quasifree peaks can be expected to get larger, and to lighter targets, where there will be less attenuation due to final state interaction.

The quasifree cross sections to be expected in nucleon-nucleus scattering can be calculated in terms of the free cross sections and the mean free paths of the nucleons in the nucleus. However, different methods of determining the mean free path have led to widely divergent results. In the simplest approximation, the mean free path of a nucleon in nuclear matter is given by the simple expression

$$\lambda=\frac{1}{\rho\sigma}\ , \tag{1}$$

where ρ is the nucleon density and σ the isospin averaged nucleon-nucleon cross sections. Taking $\rho=0.17$ fm^{-3}, λ would, in a nucleus with equal numbers of neutrons and protons, reach a maximum of about 2 fm at a nucleon (laboratory) energy of 400 MeV and be down to about 1.5 fm at 150 MeV. Pauli blocking can be expected to increase this estimate of the mean free path by about a factor of 1.5 at 150 MeV and by lesser amounts at higher energies. A value for the mean free path can also be obtained from the imaginary part of the nucleon-nucleus optical model potential using the expression

$$\lambda=\frac{-\mu h}{2W}\ , \tag{2}$$

where W is the imaginary part of the potential and μ is the velocity of nucleons in nuclear matter. The values of the imaginary potential found by Nadasen *et al.*[7] imply a mean free path of 6–9 fm.

It is possible to infer the attenuation of nucleons in nuclei from cross section measurements. An expression has been derived[8] for the reaction cross section:

$$\sigma_R=\pi r^2\left[1-\frac{V_c}{E}\right](1-T)\ , \tag{3}$$

where $r=r_N=\lambda$; r_N is the nuclear radius, V is the Coulomb energy at nuclear surface, and T is the nuclear transmission

$$T=\frac{1-\left[1+\frac{r}{\lambda}\right]e^{-2(r/\lambda)}}{2\left[\frac{r}{\lambda}\right]^2}.$$

Using nuclear radii obtained from optical model fits and measured reaction cross sections Nadasen *et al.*[7] found $\lambda=5.2\pm1$ fm. However, Dymarz and Kohmura[9] have pointed out that when the nuclear transmission is small, a small change in radius will necessitate a large change in the mean free path in order for Eq. (3) to reproduce the same reaction cross section. Since for the lightest nucleus studied by Nadasen *et al.*, ^{40}Ca, $T\approx25\%$, the point raised by Dymarz and Kohmura appears to be well taken. Varying both the nuclear radius and the mean free path in order to fit both the reaction and the total cross section, Dymarz and Kohmura obtained mean free paths of ≈3 fm in the 40–200 MeV region and about 2 fm between 400 and 1000 MeV. From the absence of quasifree peaks in their inclusive proton spectra, Segel *et al.* concluded that the attenuation of the quasifree peaks required a mean free path at 164 eV smaller than about 3.5 fm.

Negele and Yazaki[10] have shown that by taking into account the nonlocality of the nucleon-nucleon potential the mean free path can be increased by a factor which decreases from about 1.5 at 50 MeV to about 1.25 at 150 MeV. When this correction is included the calculated mean free path is brought into near agreement with the large values that are inferred from the optical potential. However, Meyer and Schwandt[11] have shown that the fitted imaginary nuclear potential, and therefore the derived mean free path, depends critically on the shape of the potential. In fact, for a shape which they consider to be better justified than the usual Woods-Saxon form, Meyer and Schwandt found mean free paths down around the 2 fm expected from the free cross sections.

In the present work a better understanding of how nucleons propagate through nuclear matter is sought by further searching for quasifree scattering in the 150 MeV region. Spectra were taken using a wide range of targets, including berylium and carbon which are lighter nuclei than any previously studied. Measurements were made over the angular range from 10° to 30°, and were thus covering smaller angles than in the previous study.[4,5] It should be noted that with 800 MeV incident protons, prominent quasifree peaks were observed[12] in the spectra, but only at angles less than 30°.

Deuteron, triton, ^{3}He, and alpha particle spectra were also obtained. The stack of solid state detectors used in the present work was superior to the NaI(Tl) crystal used previously,[5] in that the energy resolution and stability were much better, and the dead layers were negligible. Higher quality spectra were therefore obtained, particularly for the $Z=2$ particles.

In the previous study,[5] significant differences were found in the spectra from ^{58}Ni and ^{62}Ni targets; the differences in the mass 3 spectra were particularly striking. In order to further ascertian the effects of neutron excess, three nickel and two tin isotopes were investigated.

EXPERIMENT

The data were taken in the large scattering chamber at the Indiana University Cyclotron Facility. Data were taken on ^{9}Be, C, ^{58}Ni, ^{62}Ni, ^{64}Ni, ^{116}Sn, ^{124}Sn, and Bi targets at an incident proton energy of 150 MeV. The particles were detected by a solid state detector stack which consisted of two Si detectors, 53 μ thick and 2010 μ thick, respectively, plus four Ge detectors, 10.7, 9, 15, and 15 mm thick, respectively. There was sufficient material to stop 150 MeV protons. Energy resolution was $\approx$400 keV.

The pulses from the four germanium detectors were summed and then treated as coming from a single detector. Plots of ΔE vs E were made, with the E signal a hardware sum of the signals from all of the detectors, and the ΔE signal either the first silicon detector or the sum of the two silicon detectors. The contours for the different particles stood out clearly and the various particle spectra were generated utilzing software cuts around each contour.

Because of the nonlinearity of the range-energy relationship even small variations in gain between the various elements in the stack can lead to sharp dips or peaks in the spectra at those energies at which the range of a given particle was just sufficient for it to enter a new element. Thus, even though the gains were matched to about 1%, glitches did appear in the spectra which were substantially eliminated by remapping the spectra allowing for these small gain changes. Only for the proton spectra were the statistical fluctuations small enough for this gain mismatch correction to have an observable effect. The spectra were also corrected for the low energy tails that result from energy being lost through nuclear reactions. The data of Cameron *et al.*[13] were utilized in making this correction, which was largest at the forward angles where scattering to the states of the target nucleus is greatest. The correction had the effect of raising the elastic peak by about 15% and at 15° the correction had the effect of removing $\approx$20% of the counts in the 40–80 MeV region. However, at 10° about $\frac{2}{3}$ of the counts at 40 MeV were attributable to low energy tails from higher energy protons entering the detector. The spectra at 10° also showed indications of significant low energy tails attributable to slit scattering of the extremely intense forward angle Coulomb scattered protons, and therefore only qualitative conclusions could be drawn from these spectra.

The effective solid angle of the system was determined by measuring proton scattering from the hydrogen in a CH_2 target. Cross sections are believed to be accurate to about 15% over and above any errors due to statistical fluctuations.

EXPERIMENTAL RESULTS

A proton spectrum, ^{58}Ni at 15°, is shown in Fig. 1. At the low end there is an evaporation peak, cut off on the low side because of the requirement that particles have sufficient energy to pass through the first silicon detector.

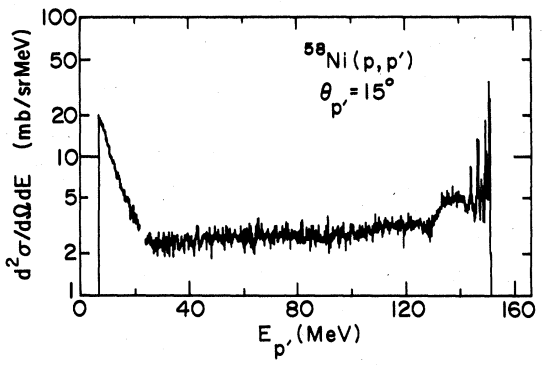

FIG. 1. Proton spectrum at 15° from ^{58}Ni. Note the log scale.

Proton evaporation was also clearly evident in the spectra from the ^{62}Ni, ^{64}Ni, and ^{116}Sn targets. The spectra from the C and, to a lesser extent, the Be targets showed a rise at the low energies which could be indicative of an evaporation peak below the detection threshold of the system. The ^{124}Sn target was substantially thicker than the others, 24 mg/cm^2, which resulted in a considerable smearing out of the evaporation peak. With the Bi target, the evaporation peak was largely surpressed, no doubt a result of the high Coulomb barrier.

In order to display the entire spectrum, a log scale is used in Fig. 1, although interest in the present work is concentrated on the continuum between the low energy evaporation protons and the high energy protons inelastically scattered to states in the target nucleus. Spectra covering this region from four of the targets are shown in Fig. 2. In order to facilitate comparisons the spectra have been drawn as lines averaging over the statistical fluctuations and a log scale has been used. For the lightest target, ^{9}Be, this region is dominated by a broad peak at about 115 MeV plus a long low-energy tail. The position of the peak is about 20 MeV below the energy expected for free nucleon-nucleon scattering. For carbon, the peak was clearly still present, but somewhat more spread out to-

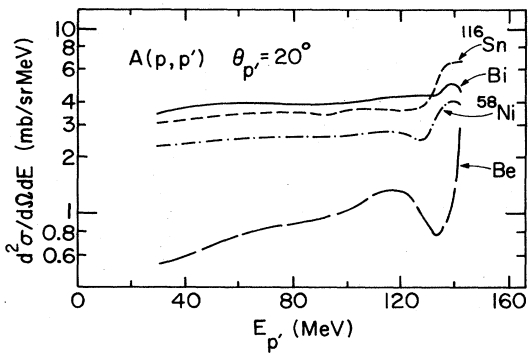

FIG. 2. Proton spectra at 20° from some of the targets. The spectra have been drawn averaging over the statistical fluctuations. Note the log scale.

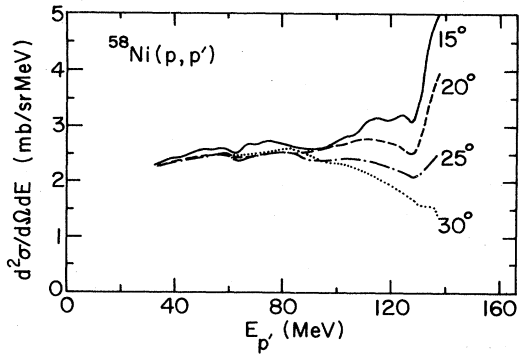

FIG. 3. Proton spectra from ^{58}Ni. The data have been smoothed.

wards the low energy side. For ^{58}Ni and heavier targets the continuum was rather flat with no clear evidence of a quasifree peak.

Proton spectra taken at the various angles are shown for one of the targets, ^{58}Ni, in Fig. 3. The data have been smoothed and the evaporation and nuclear scattering regions, both of which are of relatively little interest in the present work, have been cut off. Inadequacies in the smoothing routine, combined with the gain mismatch, could produce dips of $\approx 5\%$ in the plotted spectra. The yield of high energy protons increases with decreasing angle, which is a continuation of the trend that was observed at larger angles.[4,5] At the smaller angles there may be some evidence of a quasifree peak, though any such peak is not clearly separated from scattering to giant resonances and other states of the target nucleus. At all angles similar shaped continua were found for all of the nickel and heavier targets, while for Be and C a quasifree peak was always present. When the results of the present experiment are combined with those previously reported,[4,6] it appears reasonable to conclude that for incident protons in the 150—200 MeV range and $A \gtrsim 50$, quasifree peaks are not a major component of the inelastic proton spectra at angles of 15° or greater.

In the previous work,[5] a difference in the proton yield from ^{58}Ni and ^{62}Ni was reported which, in view of the experimental error, was of doubtful significance. Figure 4 shows spectra over the energy region of interest from the three nickel isotopes. The spectra are similar and any

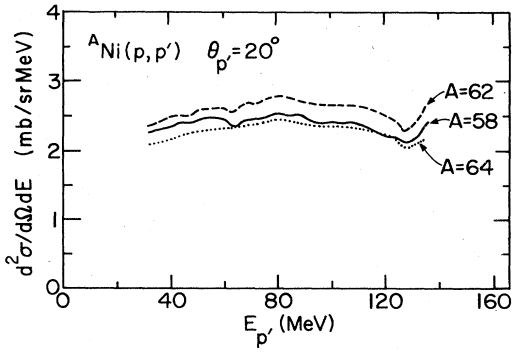

FIG. 4. Proton spectra, at 20°, from the various nickel isotopes. The data have been smoothed.

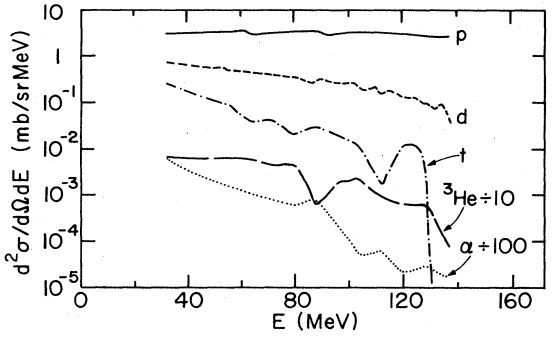

FIG. 5. Spectra of the various particles from ^{116}Sn at 25°. The data have been smoothed.

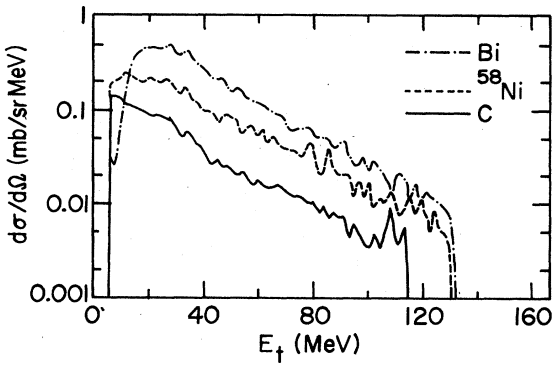

FIG. 6. Smoothed triton spectra from C, ^{58}Ni, and Bi at 25°. The triton spectra from the other targets were similar in shape to these and, in fact, for each type of outgoing particles, the shape of the spectrum varied little with target.

differences in magnitude are within the ≈15% uncertainty in the target thicknesses. Furthermore, there is no discernable trend in the data. The proton spectra from the two Sn targets were also quite similar.

Spectra of deuterons, tritons, ^{3}He, and alphas from one target, ^{116}Sn, at one angle, 25°, are shown in Fig. 5. As observed previously,[5] the proton yield is ≈10 times the deuteron yield; the triton yield is down by about another factor of 10, and the ^{3}He and alpha particle yields are roughly comparable to the triton yield. In general, the greater the mass of the outgoing particle the more rapidly the yield falls off with increasing particle energy, though the ^{3}He spectrum is flatter than the triton spectrum. For each particle the spectral shape over the continuum region was roughly independent of target.

Yields of the various particles, summed over the energy region from 40 to 120 MeV, are tabulated in Table I. The energy region was chosen to avoid evaporation particles at the one end and excitation of bound states and of giant resonances at the other. Of course, caution must be excercised in drawing conclusions from data taken at a single angle. However, the previous work[5] showed that the angular distribution of any of the outgoing particles is rather independent of A, particularly at the more forward angles where the yield of fast particles is greatest, and the present work supports this contention. In fact, the angular distribution of the fact continuum is approximately the same for all of the outgoing particles. The shapes of the various particle spectra differ, as can be seen in Fig. 5,

TABLE I. Yields at 25°, in mb/sr, of the various particles with outgoing energy between 40 and 120 MeV.

	p	d	t	^{3}He	α
^{9}Be	417	54.8	6.33	8.70	7.07
^{12}C	446	57.5	5.13	9.91	10.1
^{58}Ni	1177	119	10.7	17.1	24.1
^{62}Ni	1282	138	15.7	16.2	26.6
^{64}Ni	1137	123	16.0	12.8	22.7
^{116}Sn	1544	162	22.4	16.6	40.3
^{124}Sn	1546	166	28.9	13.3	33.7
^{209}Bi	1861	195	37.5	16.0	66.2

and therefore the relative yields of the various particles can depend on the energy interval over which the spectra are summed. However, as illustrated in Fig. 6, the shape of the spectrum for a given particle is substantially independent of target.

In view of the fact that both the energy and the angular distribution of each outgoing particle is insensitive to the target, the yields over a given energy region at a single angle give a good picture of the overall target dependence of each particle's yield. Over the entire mass region, the dependence on yield with A is noticeably weaker for ^{3}He than for the other particles. If the yields are fitted to a power law, $Y=kA^{\alpha}$, and if only the region from ^{58}Ni to ^{209}Bi is considered, the best fit finds the ^{3}He yield virtually independent of A, $\alpha=0.004$. In contrast, the triton yield over the same region varies as $A^{0.85}$.

When comparing spectra from different isotopes, the most significant effects are seen in the triton and ^{3}He spectra. For particles with energies >40 MeV, ^{3}He than tritons are produced from ^{58}Ni while it is the other way around with the ^{64}Ni target. Between these two isotopes the neutron to proton ratio changes by 28%, while the ratio of ^{3}He to triton yield changes by a factor of 2. A simi-

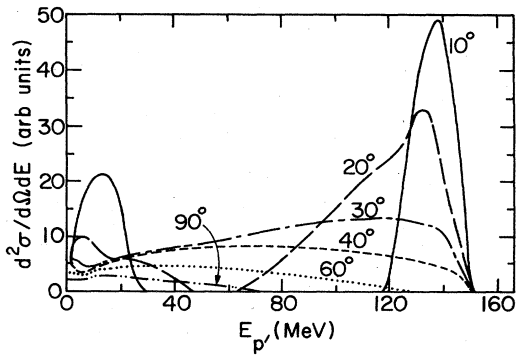

FIG. 7. Calculated proton spectra from the scattering of 150 MeV protons by a Fermi gas, $p_{max}=220$ MeV/c, consisting of equal numbers of protons and neutrons.

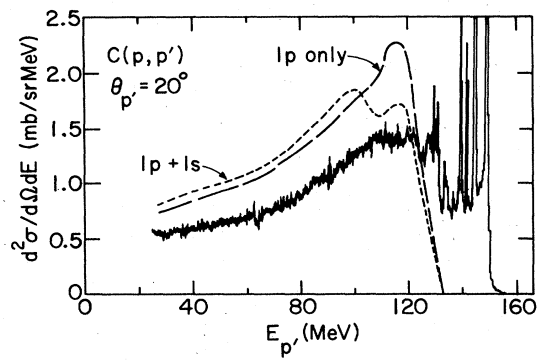

FIG. 8. Proton spectrum from C at 20° compared with spectra calculated assuming a single scattering from a Fermi gas.

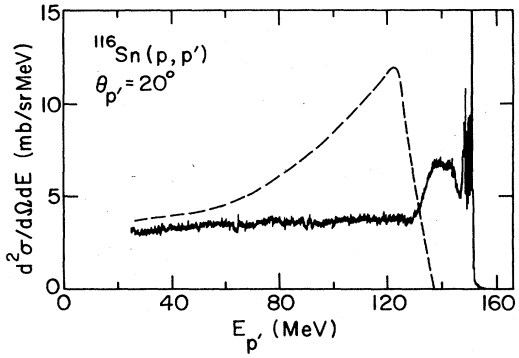

FIG. 9. Proton spectrum from ^{116}Sn at 20° compared with the spectrum calculated assuming a single scattering from a Fermi gas.

lar effect is present in the yields of mass 3 particles from the tin isotopes.

DISCUSSION OF RESULTS

Any nucleon-nucleon scattering peak would be broadened by the motion of the nucleons in the nucleus and in order to estimate this broadening, a calculation was performed assuming a Fermi gas nucleus. The methods given by Moniz[14] were used and, while the calculation is basically classical, Pauli blocking is allowed for. Calculations were performed separately for a neutron and for a proton target gas and the results combined. The Fermi momentum in the nucleus was taken to be 220 MeV/c. Free nucleon-nucleon cross sections were obtained from Arnot.[15] Figure 7 shows the results of such a calculation for a nucleus consisting of equal numbers of neutrons and protons, all with no binding energy. It can be seen that down to 10° (laboratory), the calculated proton scattering peak gets higher as the angle gets smaller, though, because of Pauli blocking, the area under the peak decreases forward of 25°. Figure 8 shows the results of a calculation for carbon along with the experimental data. Binding energies of 17.5 MeV for the $1p$ shell and 38.1 MeV for the $1s$ shell were taken from the work of Mougey *et al.*[16] Also shown in Fig. 8 is the calculated spectrum for scattering from the $1p$ shell nucleons alone (i.e., 17.5 MeV binding energy). Both calculated curves are normalized by setting the total calculated cross section equal to the total reaction cross section, which has been measured[17] to be 215 mb. Actually, the shape of the spectrum at 20° was best fit when $1s$ shell nucleons were taken to be about 40% as effective in scattering as $1p$ shell nucleons.

Figure 9 shows a comparison of the results of the Fermi gas calculation with the data for ^{116}Sn at 20°, which is the smallest angle at which the quasifree peak could be expected to be separated from the inelastic scattering of states in the target nucleus. The calculated spectrum is for scattering by nucleons bound by 13 MeV, a value indicated by the position of the quasifree peak that is observed in 400 MeV inclusive proton spectra.[18] Again, the total calculated cross section was set equal to the total reaction cross section which was taken to be[19] $\sigma_R=\pi r_i^2$, $r_i=1.25A^{1/3}$ fm. Under these assumptions it can be seen that the quasifree peak must be attenuated by at least a factor of 3. In Table II, the attenuations of the calculated peaks that are needed in order to fit, or be consistent with, the data at 20°, are listed. As expected, the heavier the nucleus, the more the peak must be attenuated.

In order to relate the attenuation of a presumed quasifree peak to the mean free path of nucleons in nuclear

TABLE II. Calculated and experimental quasifree peaks. Quasifree scattering was calculated using a Fermi gas model normalized to the total reaction cross section, taken to be 172 mb for Be, 215 mb for C, and $\pi r_i^{2/3}$, $r_i=1.25A^{1/3}$ fm, for the heavier targets. The second column gives the attenuation of the calculated peak that is required in order to be consistent with experiment. The third column gives the ratio of nucleon mean free path to the radius of a uniform sphere (Fig. 10) that this attenuation implies. The fourth column is the third column multiplied by $A^{1/3}$.

Nucleus	Attenuation	$\frac{\text{Mean free path}}{\text{nuclear radius}}$	$\frac{\text{Mean free path}}{\text{nuclear radius}}\times A^{1/3}$
Be	0.75	2.5	5.2
C	0.63	1.6	3.7
^{58}Ni	<0.37	<0.76	<2.9
^{62}Ni	<0.43	<0.88	<3.5
^{64}Ni	<0.35	<0.72	<2.9
^{116}Sn	<0.32	<0.67	<3.2
^{124}Sn	<0.32	<0.67	<3.4
^{209}Be	<0.25	<0.53	<3.2

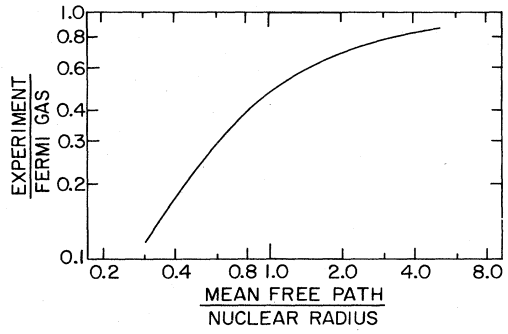

FIG. 10. Calculated attenuation assuming that the nucleus is a uniform sphere.

matter a calculation was performed in which the nucleons were assumed to be attenuated as $e^{-l/\lambda}$, with λ being the nucleon mean free path. The attenuation of the quasifree peak would then be the ratio of the number of nucleons emerging at a given angle to the number initially scattered through that angle. The nucleus was considered to be a uniform density sphere and thus the attenuation was solely a function of the ratio of the mean free path to the nuclear radius. Figure 10 shows the calculated attenuation of the quasifree peak. Within the framework of this calculation, the spectrum from ^{116}Sn at 20°, shown in Fig. 9, would imply that the mean free path is less than $\frac{2}{3}$ of the nuclear radius (Table II). The lighter the nucleus, the more stringent the limit that can be placed on the mean free path. For the nickel isotopes a mean free path of no more than about 75% of the nuclear radius is implied, which would put an upper limit of about 3.5 fm on the mean free path. For carbon and berylium, actual attenuations, rather than upper limits, are determined, but for these light nuclei a uniform sphere is such a poor approximation that the value extracted for the mean free path cannot be taken too seriously.

There are other methods by which the quasifree scattering can be calculated. Cascade calculations have been performed in this energy region and, as previously noted,[5] predict much too prominent a quasifree peak. Distorted wave impulse approximation calculations might be illuminating but no such calculations for quasifree scattering appear to have been done in this energy region.

Significant trends can be discerned in the spectra of the heavier particles and it should be possible to extract useful nuclear information from these. Unfortunately, however, at the present time there is no computational framework that can be utilized in relating the data to nuclear properties. Hopefully, the availability of good data will spur calculational efforts.

This work was supported by the National Science Foundation.

*Present address: Institute for Nuclear Research, Warsaw, Poland.

[1]N. S. Wall and P. R. Roos, Phys. Rev. **150**, 811 (1966).
[2]J. W. Wachter, W. R. Burrus, and W. A. Gibson, Phys. Rev. **161**, 971 (1967).
[3]R. W. Peelle, T. A. Love, N. W. Hill, and R. T. Santoro, Phys. Rev. **167**, 981 (1968).
[4]T. Chen, R. E. Segel, P. T. Debevec, J. Wiggins, P. P. Singh, and J. V. Maher, Phys. Lett. **130B**, 192 (1981).
[5]R. E. Segel, T. Chen, L. L. Rutledge, Jr., J. V. Maher, J. Wiggins, P. P. Singh, and P. T. Debevec, Phys. Rev. C **26**, 2424 (1982).
[6]H. Machner, D. Protic, G. Riepe, J. P. Didelez, N. Frascaria, E. Gerlic, E. Hourani, and M. Morlet, Phys. Lett. **138B**, 39 (1984).
[7]A. Nadasen, P. Schwandt, P. P. Singh, W. W. Jacobs, A. D. Bacher, P. T. Debevec, M. D. Kaitchuk, and J. T. Meek, Phys. Rev. C **23**, 1023 (1981).
[8]H. A. Bethe, Phys. Rev. **57**, 1125 (1940); M. M. Shapiro, *ibid.* **90**, 171 (1953).
[9]R. Dymarz and T. Kohmura, Phys. Lett. **124B**, 446 (1983).
[10]J. W. Negele and K. Yazaki, Phys. Rev. Lett. **47**, 71 (1981).
[11]H. O. Meyer and P. Schwandt, Phys. Lett. **107B**, 353 (1981).
[12]R. E. Chrien, T. J. Kreger, R. J. Sutter, M. May, H. Palevsky, R. L. Stearns, T. Kozlowski, and T. Bauer, Phys. Rev. C **21**, 1014 (1980).
[13]J. M. Cameron, P. Kitching, R. H. McCamis, C. A. Miller, G. A. Moss, J. G. Rogers, G. Roy, A. W. Stetz, C. A. Goulding, and W. T. H. van Oers, Nucl. Instrum. Methods **143**, 399 (1977).
[14]E. Moniz, Phys. Rev. **184**, 1154 (1969).
[15]R. A. Arnot, private communication. We thank Dr. Arndt for providing a tape of compiled cross sections.
[16]J. Mougey, M. Bernheim, A. Bussiere, A. Gillebert, Phan Xuan Ho, M. Priou, D. Royer, I. Sick, and G. J. Wagner, Nucl. Phys. **A262**, 461 (1976).
[17]H. O. Meyer, P. Schwandt, W. W. Jacobs, and J. R. Hall, Phys. Rev. C **27**, 459 (1983).
[18]R. E. Segel, A. A. Hassan, S. M. Levenson, K. P. Jackson, P. P. Singh, L. W. Swenson, J. Tinsley, and J. Lisantti, Bull. Am. Phys. Soc. **29**, 627 (1984); and private communication.
[19]P. Schwandt, *Proceedings of the RCNP Symposium on Light Ion Reaction Mechanisms, Osaka, Japan, 1983,* edited by H. Ogata, T. Kammuri, and I. Katayma (RCNP, Osaka, 1983), p. 3.